Low temperature texture development in $Nd_2Fe_{14}B$/α-Fe nanocomposite magnets via equal channel angular pressing

L. Besley, J. S. Garitaonandia, A. Molotnikov, H. Kishimoto, A. Kato, C. Davies, and K. Suzuki

Citation: AIP Advances **8**, 056219 (2018); doi: 10.1063/1.5006359
View online: https://doi.org/10.1063/1.5006359
View Table of Contents: http://aip.scitation.org/toc/adv/8/5
Published by the American Institute of Physics

Low temperature texture development in $Nd_2Fe_{14}B/\alpha$-Fe nanocomposite magnets via equal channel angular pressing

L. Besley,[1,a] J. S. Garitaonandia,[2] A. Molotnikov,[1] H. Kishimoto,[3] A. Kato,[3] C. Davies,[4] and K. Suzuki[1]

[1]*Department of Materials Science and Engineering, Monash University, 3800 Melbourne, Australia*
[2]*Department of Applied Physics II Faculty of Science and Technology University of the Basque Country UPV/EHU, Sarriena, 48940 Leioa, Bilbao, Basque Country (Spain)*
[3]*Toyota Motor Corporation, Mishuku, Susono, Shizuoka 410-1193, Japan*
[4]*Department of Mechanical and Aerospace Engineering, Monash University, 3800 Melbourne, Australia*

(Presented 7 November 2017; received 25 September 2017; accepted 16 November 2017; published online 5 January 2018)

While suitable texture has been developed in $Nd_2Fe_{14}B/\alpha$-Fe nanocomposites via thermomechanical processing methods such as die upsetting by incorporating low melting point eutectic Nd-Cu additives, significant grain coarsening occurs during this process due to the high temperature and long timescales involved, resulting in a loss of exchange coupling. Equal channel angular pressing (ECAP) is a severe plastic deformation technique which has been successfully used to produce a suitable texture in single-phase $Nd_2Fe_{14}B$ at temperatures on the order of 500°C while preserving grain sizes on the order of 20-30nm. We investigate the development of texture in a commercial $Nd_2Fe_{14}B/\alpha$-Fe nanocomposite alloy with added $Nd_{90}Cu_{10}$ produced via ECAP and then characterise it using texture x-ray diffraction and magnetic measurements. It is found that initial texture can be developed in this nanocomposite system at T = 520°C via ECAP. The average grain size of $Nd_2Fe_{14}B$ as measured via X-ray diffraction after ECAP remains below 50nm with a developed texture. The effect of varying the amount of $Nd_{90}Cu_{10}$ additive is also investigated. It is found that with decreasing $Nd_{90}Cu_{10}$, the degree of texture is reduced while the volume fraction of α-Fe increases. This work demonstrates the development of texture in nanocomposite $Nd_2Fe_{14}B/\alpha$-Fe with Nd-Cu additives whilst maintaining a grain size of approximately 50nm. https://doi.org/10.1063/1.5006359

I. INTRODUCTION

$Nd_2Fe_{14}B/\alpha$-Fe nanocomposite magnets promise excellent performance with high theoretical maximum energy products due to the effects of exchange coupling.[1–3] In order to realise the full potential of nanocomposites, texture must be developed without losing exchange coupling. While texture can be developed in nanocomposites via thermomechanical processing such as die upsetting and the incorporation of low melting point eutectic Nd-rich additives (such as Nd-Cu and Nd-Ga) that help improve the workability and facilitate texture development in these materials,[4–8] the temperature and timescale required for such processing causes grain coarsening, resulting in a final microstructure with grain sizes on the order of 200-1000nm,[8] well above the predicted exchange length for $Nd_2Fe_{14}B$.[1] Other works show that exchange coupling may be observed experimentally at grain sizes slightly above this limit, but still on the order of 30-50nm.[9,10] In order to maintain

[a]Electronic mail: Luke.Besley@monash.edu

exchange coupling in larger scale nanocomposites, bulk processing routes which do not incur grain growth must be investigated. Equal Channel Angular Pressing (ECAP) has been used successfully to develop texture in $Nd_2Fe_{14}B$-based materials without appreciable grain growth.[11,12] In this work, $Nd_2Fe_{14}B/\alpha$-Fe nanocomposite materials are combined with Nd-Cu additives to develop suitable texture via ECAP while maintaining a grain size of approximately 50nm.

II. METHODS

Elements with >99.99% purity were arc melted with composition $Nd_{90}Cu_{10}$. Ingots were then melt spun with a wheel speed of 40 m/s and pulverised into particles of $< 250\mu$m under Ar. The $Nd_{90}Cu_{10}$ was then added to a commercial hypo-stoichiometric $Nd_{7.91}Pr_{2.68}Fe_{84}B_{5.41}$ alloy[13] (herein referred to as MQP15-7), at a ratio of $x_{[NdCu]}$=4, 7, and 10 wt%, and the two powders were subsequently mixed under Ar. Mixed powders were then pre-compacted under Ar at T = 550°C under a pressure of $\sigma \approx 125$ MPa and then annealed at T = 550°C under a vacuum of 10^{-3} Pa over a range of times (t). After annealing, the samples were then processed via ECAP at T = 520°C (unless otherwise stated). Further details of the ECAP process and subsequent sample characterisation are described in previous work.[12] Scanning Electron Microscopy images were taken with a JEOL 7001-F. Estimations of grain size were calculated from X-ray diffraction patterns using the integral breadth method.[14] ^{57}Fe Mössbauer spectra were acquired at room temperature using a constant acceleration transmission spectrometer with a ^{57}CoRh source.

III. RESULTS AND DISCUSSION

A. The effect of annealing treatment

Fig. 1 shows the change in M-H curves with varying annealing time, while Table I shows changes in $|BH|_{Max}$, ΔM_r and grain size. Initially, without pre-annealing (i.e. t=0h), ΔM_r and $|BH|_{Max}$ are quite low. With the a pre-annealing treatment, $|BH|_{Max}$ and M_r increase. As t further increases, H_c begins to significantly begins to significantly improve as well. However, beyond t=25h, H_c, $|BH|_{Max}$ and M_r begin to I also shows the change in grain size with varying annealing time. Even at the longest annealing time, the grain size tends to remain well below 100nm. Fig. 2 shows pole figures characterising the distribution of (001) planes after ECAP throughout the plane normal to the exit channel with varying annealing times (PD = pressing direction, TD = transverse direction). As t increases, the maximum m.r.d.[15] observed increases to a maximum at t=25h. The most prominent texture is observable in c), where the (001) basal plane aligns parallel to the shear direction produced in ECAP, distributed approximately 40° away from the exit direction, normal to the easy axis (c-axis). This behaviour of (001) planes in $Nd_2Fe_{14}B$ aligning parallel to the planes of shear in plastic deformation is consistent with previous studies involving ECAP of $Nd_2Fe_{14}B$[11] and die upsetting.[16] Consistent with the trends observed in Fig. 1 and Table I, the maximum m.r.d. increases as t increases until t=25h where the strongest texture is observed and decreases afterwards.

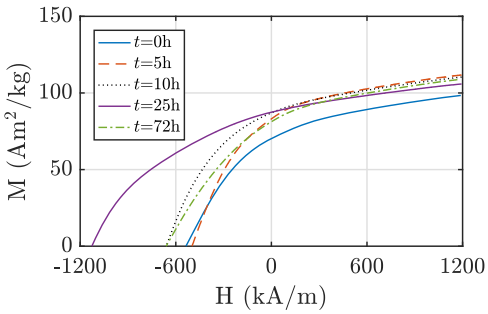

FIG. 1. Demagnetisation curves of parallel direction field-aligned powders of 15-7+10wt% after ECAP where t = annealing time for a) t=5h, b) t=10h, c) t=25h, d) t=72h.

TABLE I. Changes in grain size of $Nd_2Fe_{14}B$+10 wt% $Nd_{90}Cu_{10}$ after ECAP.[a]

$t_{Annealing}$(h)	ΔM_r[b]	$\|BH\|_{Max}$[c]	Grain Size (nm)
0	5.5 (0.2)	57 (4)	24(2)
5	14.3 (0.6)	73 (4)	39(2)
10	16.1 (0.6)	93 (6)	41(2)
25	21.8 (0.8)	108 (6)	52(2)
72	13.4 (0.6)	75 (4)	54(4)

[a]numbers in parentheses reflect absolute error.
[b](Am^2/kg).
[c](kJ/m^3).

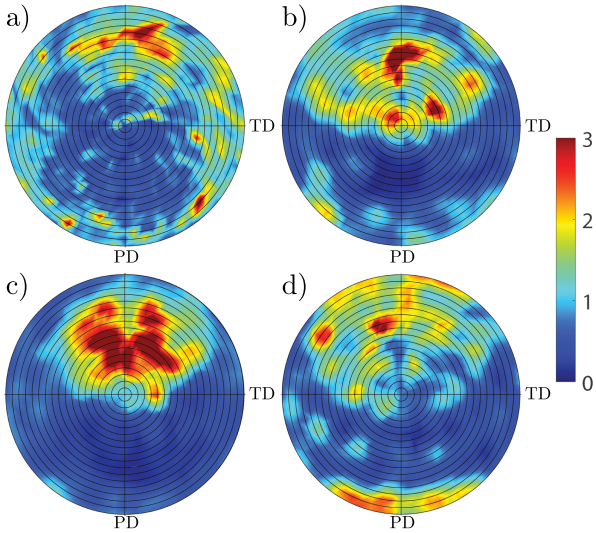

FIG. 2. Pole Figures showing the distribution of the (001) plane taken from the cross section normal to the exit direction in ECAP for a) t=5h, b) t=10h, c) t=25h, and d) t=72h. ↓=pressing direction (PD), ↔=transverse direction (TD).

Fig. 3 shows the fracture surface observed via SEM after ECAP of a sample that had been annealed for t=25h with $x_{[NdCu]}$=7wt%. Although a range of larger (i.e. >100nm) grains can be observed, many smaller grains are clearly visible, consistent with the mean grain size estimated by XRD in Table I. The variation in Table I suggests that at first, the texture is quite weak after ECAP until a sufficient pre-annealing treatment is introduced, after which texture strength increases appreciably. In previous trials involving the processing of hyper-stoichiometric $Nd_2Fe_{14}B$ with a well-dispersed rare earth-rich grain boundary phase, the timescale of processing via ECAP is adequate to develop a strong texture.[11,12] However, since ECAP generally occurs on a much shorter

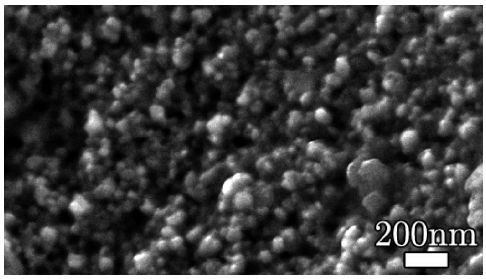

FIG. 3. Fracture surface of 15-7+7wt%$Nd_{90}Cu_{10}$ after ECAP obtained by scanning electron microscopy.

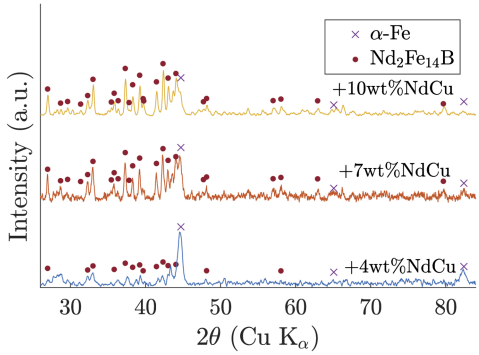

FIG. 4. 2θ scans of 15-7 after ECAP with varying wt% with varying additions of $Nd_{90}Cu_{10}$. Prominent peaks belonging to α-Fe and $Nd_2Fe_{14}B$ phases are labeled.

timescale and lower temperature than die-upsetting (on the order of ~100s), the processing of hypo-stoichiometric $Nd_2Fe_{14}B/\alpha$-Fe with rare earth-rich additives must then require additional mechanisms such as annealing to aid the diffusion of the Nd-rich phase into the grain boundary. Without such additional mechanisms, the degree of $Nd_{90}Cu_{10}$ diffusion after ECAP is severely reduced compared to that of die upsetting. Based on the diffusion coefficients[17] of ^{147}Nd, t=25h corresponds to a diffusion length of approximately 300μm, which just exceeds the average size of precursor powders (<250μm) in these experiments. After t=25h, further increases in pre-annealing time result in a decrease in texture strength and $|BH|_{Max}$, supporting the notion that t=25h is sufficient for adequate $Nd_{90}Cu_{10}$ diffusion.

B. The effect of varying $Nd_{90}Cu_{10}$ content

Given the optimal properties at t=25h, compositions with $x_{[NdCu]}$=4, 7, and 10wt% additions were investigated with this fixed annealing time.

Fig. 4 shows XRD patterns for each composition after ECAP. When $x_{[NdCu]}$=4wt%, both the (110) and (211) peaks belonging to the α-Fe phase become very large. When $x_{[NdCu]}$=7wt%, the (110) and (211) peaks decrease significantly, but still are quite prominent. At $x_{[NdCu]}$=10wt%, the (110) and (211) α-Fe peaks have almost disappeared.

Fig. 5 shows demagnetisation curves of field-aligned powders measured both parallel (solid curves) and perpendicular (dotted curves) to the applied field for $x_{[NdCu]}$=4wt%, 7wt%, 7wt% with T_{ECAP} = 550°C and 10wt%. At $x_{[NdCu]}$=4wt%, H_c, M_r and $|BH|_{Max}$ have decreased significantly. Nonetheless, an appreciable ΔM_r still remains. As $x_{[NdCu]}$ increases, M_s systematically decreases and appreciable M_r and $|BH|_{Max}$ are observed. The shape of the demagnetisation curve remains relatively smooth, suggesting a reasonable preservation of exchange coupling for samples c) and d).[18] Fig. 6 shows (001) pole figures for these same compositions and processing conditions. The observable

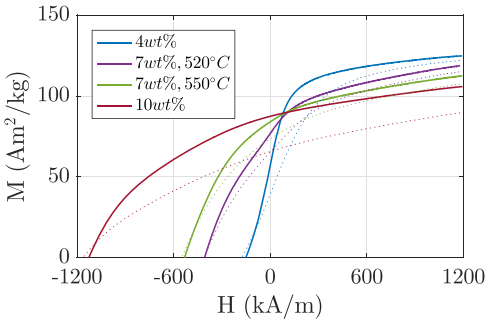

FIG. 5. Demagnetisation curves of field-aligned powder measured both parallel (solid) and perpendicular (dotted) to the applied field direction for $x_{[NdCu]}$= a) 4wt%, b) 7wt%, c) 7wt% with T = 550°C and d) 10wt%.

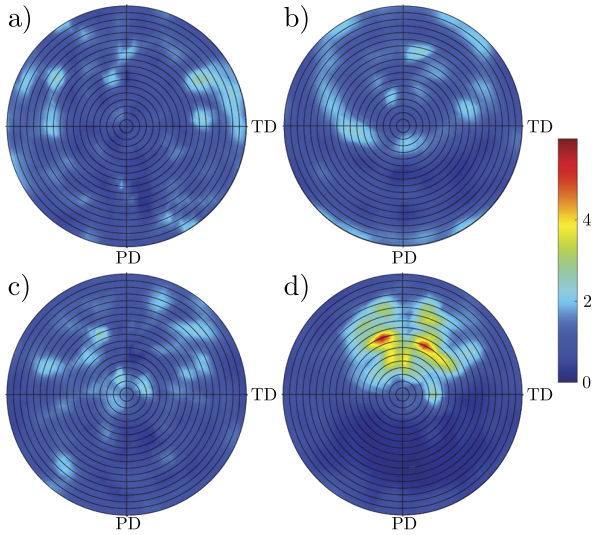

FIG. 6. (001) pole figures from the plane normal to the exit direction (PD=Pressing Direction, TD=Transverse direction) for $x_{[NdCu]}$= a) 4wt%, b) 7wt%, c) 7wt% with T_{ECAP} = 550°C and d) 10wt%.

trend is similar to Fig. 5. The texture is strongest when $x_{[NdCu]}$=10wt% and decreases with decreasing $x_{[NdCu]}$ as the (001) plane alignment becomes increasingly isotropic. For $x_{[NdCu]}$ = 7wt%, the effect of increasing temperature during ECAP was also investigated, and can be observed in Fig. 5, as well as the difference between b) and c) in Fig. 6. There is a slight improvement in H_c, $|BH|_{Max}$, and M_r, while M_s shows a slight decrease. These trends are similar to the trend between $x_{[NdCu]}$=7 and 10wt%, the latter of which displays the strongest texture and least α-Fe. This suggests that further increasing T_{ECAP} could further enhance texture and $|BH|_{Max}$.

Table II shows the change in composition of $W_{[\alpha-Fe]}$ after ECAP with varying $x_{[NdCu]}$, as calculated by peak-fitting of Mössbauer spectra. An example of one of the Mössbauer spectra used for calculation is shown in Fig 7. When $x_{[NdCu]}$=4wt%, $W_{[\alpha-Fe]}$ is as large as ~24wt%, and then reduces to 0 as $x_{[NdCu]}$ is increased. These results are consistent with the trend observable in Fig. 4. At $x_{[NdCu]}$=4wt%, peaks belonging to the α-Fe phase are quite prominent, and gradually reduce, to the point of almost entirely disappearing as $x_{[NdCu]}$ is increased.

While an appreciable ΔM_r is kept even at $x_{[NdCu]}$=4wt%, H_c and $|BH|_{max}$ have significantly decreased, and the texture has appreciably diminished. Given the presence of a rare earth-rich eutectic grain boundary phase is generally required for the formation of texture in $Nd_2Fe_{14}B$,[4,8] such a decrease in strength of texture is expected when the amount of grain boundary phase is reduced. Nonetheless, a slight texture still remains at $x_{[NdCu]}$=4wt%, even when a significant amount of α-Fe is present. It is also observable in Fig. 5 that as $W_{[\alpha-Fe]}$ increases, M_s also increases. The shape of the demagnetisation curve remains relatively smooth in the second quadrant, which may indicate a preservation of exchange coupling, however when $x_{[NdCu]}$=10 wt%, $W_{[\alpha-Fe]}$ is very low and this shape may be explainable by a single hard phase $Nd_2Fe_{14}B$ composition rather than exchange coupling between hard and soft phases. Additionally, at $x_{[NdCu]}$=4wt% a very significant loss of coercivity

TABLE II. The effect on composition (wt% α-Fe) after ECAP of varying wt% $Nd_{90}Cu_{10}$ added, as determined by Mössbauer spectroscopy.

wt% $Nd_{90}Cu_{10}$	wt% α-Fe (Mössbauer)[a]
4	24(2)
7	15(2)
10	0(2)

[a]numbers in parentheses reflect absolute error.

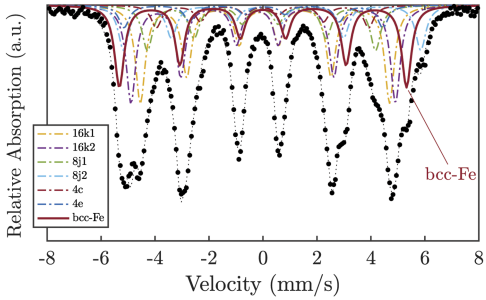

FIG. 7. Mössbauer spectra for $x_{[NdCu]}$=7wt% after ECAP.

is observed. Ideally, a well exchange-coupled nanocomposite should allow for much larger amounts[2,19] of soft phase before significant losses in coercivity are observed, but even at $W_{[\alpha-Fe]} \approx 24$wt%, significant coercivity loss is observed in these experiments, suggesting that some exchange coupling may have been lost.

IV. CONCLUSION

Initial texture can be produced in hypo-stoichiometric $Nd_2Fe_{14}B/\alpha$-Fe nanocomposites with Nd-Cu based additives at a suitably low temperature with both a grain size below 100nm and a significant amount of α-Fe remaining after thermomechanical processing. Given the short timescale of ECAP, a pre-annealing treatment aids diffusion of the Nd-Cu grain-boundary phase, further enhancing the texture. The degree of texture increases as the amount of $Nd_{90}Cu_{10}$ added increases, however the amount of residual α-Fe also decreases to almost zero as more $Nd_{90}Cu_{10}$ is added. Future work would involve further in-depth analysis of the nanostructure and further optimisation of $Nd_{90}Cu_{10}$ diffusion to further enhance texture and increase $|BH|_{Max}$ while retaining α-Fe. Nonetheless, slight texture can be developed still with an appreciable amount of α-Fe remaining without incurring significant grain growth, all important necessary preconditions that must be maintained in view of the development of bulk-scale anisotropic exchange coupled $Nd_2Fe_{14}B/\alpha$-Fe nanocomposites.

ACKNOWLEDGMENTS

The authors acknowledge use of facilities within the Monash Center for Electron Microscopy. This paper is based on results obtained from the future pioneering program "*development of magnetic material technology for high-efficiency motors*", commissioned by the New Energy and Industrial Technology Development Organization (NEDO).

[1] E. F. Kneller and R. Hawig, IEEE Transactions on Magnetics **27**, 3560 (1991).
[2] H. Fukunaga and H. Nakamura, IEEE Transactions on Magnetics **36**, 3285 (2000).
[3] I. Betancourt and H. A. Davies, Materials Science and Technology **26**, 5 (2010).
[4] L. Li and C. D. Graham, Journal of Applied Physics **67**, 4756 (1990).
[5] A. Kirchner, D. Hinz, V. Panchanathan, O. Gutfleisch, K. H. Müller, and L. Schultz, IEEE Transactions on Magnetics **36**, 3288 (2000).
[6] A. Kirchner, J. Thomas, O. Gutfleisch, D. Hinz, K. H. Müller, and L. Schultz, Journal of Alloys and Compounds **365**, 286 (2004).
[7] H. W. Kwon and J. H. Yu, IEEE Transactions on Magnetics **45**, 4435 (2009).
[8] X. Tang, R. Chen, W. Yin, J. Wang, X. Tang, D. Lee, and A. Yan, Applied Physics Letters **102**, 072409 (2013).
[9] G. C. Hadjipanayis and L. Withanawasam, IEEE Transactions on Magnetics **31**, 3596 (1995).
[10] S. D. Li, W. S. Sun, and M. X. Quan, Materials Letters **30**, 351 (1997).
[11] E. Onal, R. Lapovok, H. Kishimoto, A. Kato, C. H. J. Davies, and K. Suzuki, Journal of Applied Physics **117**, 17A742 (2015).
[12] L. Besley, H. Zhang, A. Molotnikov, H. Kishimoto, A. Kato, C. Davies, and K. Suzuki, IOP Conference Series: Materials Science and Engineering **194**, 012043 (2017).
[13] A commercially available alloy from Magnequench.
[14] T. H. de Keijser, J. I. Langford, E. J. Mittemeijer, and A. B. P. Vogels, Journal of Applied Crystallography **15**, 308 (1982).

[15] M.r.d.=Multiple of Random Distribution.
[16] V. Panchanathan, Journal of Materials Engineering **11**, 51 (1989).
[17] W. Sprengel, S. Herth, V. Barbe, H. E. Schaefer, T. Wejrzanowski, O. Gutfleisch, and R. Wurschum, Journal of Applied Physics **98**, 074314 (2005).
[18] L. Xu, Y. Liu, D. Guo, L. Zhou, F. Wang, H. Zhang, and X. Zhang, Journal of Physics D: Applied Physics **44**, 355002 (2011).
[19] T. Schrefl, J. Fidler, and H. Kronmüller, Physical Review B **49**, 6100 (1994).